Suppression of the commensurate spin-Peierls state in Sc-doped $Ti_{1-x}Sc_xOCl$ ($x=0.0$, 0.01, and 0.03)

J. P. Clancy,[1] B. D. Gaulin,[1,2] J. P. Castellan,[1] K. C. Rule,[1] and F. C. Chou[3]
[1]*Department of Physics and Astronomy, McMaster University, Hamilton, Ontario, Canada L8S 4M1*
[2]*Canadian Institute for Advanced Research, 180 Dundas Street W., Toronto, Ontario, Canada M5G 1Z8*
[3]*Center for Condensed Matter Sciences, National Taiwan University, Taipei 106, Taiwan*
(Received 6 June 2008; published 31 July 2008)

We have performed x-ray scattering measurements on single crystals of the doped spin-Peierls compound $Ti_{1-x}Sc_xOCl$ ($x=0,0.01,0.03$). These measurements reveal that the presence of nonmagnetic dopants has a profound effect on the unconventional spin-Peierls behavior of this system, even at concentrations as low as 1%. Sc doping suppresses commensurate fluctuations in the pseudogap and incommensurate spin-Peierls phases of TiOCl and prevents the formation of a long-range ordered spin-Peierls state. Broad incommensurate scattering develops in the doped compounds near $T_{c2}\sim 93$ K and persists down to base temperature (~ 7 K) with no evidence of a lock-in transition. The width of the incommensurate dimerization peaks indicates short correlation lengths on the order of ~ 12 Å below T_{c2}. The intensity of the incommensurate scattering is significantly reduced at higher Sc concentrations, indicating that the size of the associated lattice displacement decreases rapidly as a function of doping.

DOI: 10.1103/PhysRevB.78.014433 PACS number(s): 75.40.−s, 78.70.Ck

I. INTRODUCTION

Low dimensional quantum magnetic systems have been a subject of great interest, particularly since the discovery of high-temperature superconductivity in the lamellar copper oxides.[1] One such family of quantum magnets are the spin-Peierls materials, quasi-one-dimensional systems which dimerize at low temperatures to form a nonmagnetic singlet ground state.[2] These systems typically possess chains of antiferromagnetically coupled spin 1/2 Heisenberg magnetic moments and strong magnetoelastic coupling.

Although the first materials to display a spin-Peierls transition were organic compounds, such as TTF-CuBDT (Ref. 2) and MEM-$(TCNQ)_2$,[3] studies of these materials were often limited by sample quality and a relatively low density of magnetic moments. The discovery of the first inorganic spin-Peierls compound, $CuGeO_3$, with $T_{SP}\sim 14$ K,[4] allowed for the growth of large, high quality single-crystal samples, as well as the opportunity to introduce a wide range of magnetic and nonmagnetic dopants into the system and study the resulting perturbations. Studies of doped $CuGeO_3$ have been carried out wherein Cu^{2+} ($S=1/2$) is substituted for Zn ($S=0$),[5–11] Mg ($S=0$),[9,12] Cd ($S=0$),[11] Ni ($S=1$),[6,9] Co ($S=3/2$),[13] and Mn ($S=5/2$),[6] or Ge^{4+} ($S=0$) is substituted for Si ($S=0$).[6,7,9,11] These experiments have revealed a rich variety of impurity-induced effects, including (i) creation of free spin 1/2 moments, (ii) reduction in correlation lengths in the spin-Peierls state, (iii) depression of the spin-Peierls transition temperature, T_{SP}, and (iv) eventual destruction of spin-Peierls order above a critical doping, x_c. Furthermore, the introduction of nonmagnetic impurities has been shown to give rise to three-dimensional antiferromagnetic order below a second transition temperature, T_N,[6,8,9,12] which either coexists with the dimerized ground state or replaces it.

Interest in spin-Peierls systems has recently been rekindled by the discovery of unconventional spin-Peierls behavior in quantum magnets based on Ti^{3+} ($3d^1$). The titanium oxyhalides Ti$O$$X$ (X=Cl,Br) have been shown to exhibit dimerized singlet ground states at low temperatures.[14,15] However, in contrast to conventional spin-Peierls materials, TiOCl and TiOBr undergo not one but two successive phase transitions with increasing temperature.[15–21] At T_{c1} there is a discontinuous phase transition between commensurate and incommensurate spin-Peierls states, followed by a continuous transition at T_{c2} to a disordered pseudogap state. In TiOCl, the pseudogap phase extends from T_{c2} up to $T^*\sim 130$ K, and throughout this range it displays an NMR signature very similar to that of the underdoped high T_c cuprate superconductors.[17] TiOCl and TiOBr are also distinguished among spin-Peierls systems due to their unusually high transition temperatures [$T_{c1}/T_{c2}\sim 63$ K/93 K and 27 K/47 K for TiOCl (Ref. 16) and TiOBr (Ref. 15), respectively] and the surprisingly large size of their singlet-triplet energy gap (~ 430 to 440 K).[17,22]

TiOCl crystallizes into the orthorhombic space-group *Pmmn* with room-temperature lattice parameters of $a=3.79$ Å, $b=3.38$ Å, and $c=8.03$ Å.[23] This structure consists of buckled Ti-O bilayers which are separated by double layers of Cl atoms and stacked vertically along the **c** axis.[16,23] Previous x-ray scattering results indicate that the lattice dimerization associated with the low-temperature commensurate spin-Peierls state occurs along the crystallographic **b** axis.[14] Between T_{c1} and T_{c2} this dimerized structure is also incommensurately modulated along both the **a** and **b** directions.[18,19] Measurements of the high-temperature magnetic susceptibility have been described by a model of spin 1/2 Heisenberg chains, with a nearest-neighbor exchange coupling of $J\sim 660$ K.[16] The effective reduction in magnetic dimensionality which occurs within the Ti-O bilayers has been attributed to the ordering of Ti d_{xy} electronic orbitals.[16]

While TiOCl and TiOBr have attracted considerable attention, little is known about the influence of impurities on the unconventional spin-Peierls ground state of compounds such

as $Ti_{1-x}Sc_xOCl$. In this material, nonmagnetic Sc^{3+} ($S=0$) ions are substituted onto Ti^{3+} ($S=1/2$) sites in analogy with Zn or Mg doping in $CuGeO_3$ and the cuprate superconductors. While the earliest bulk characterization of $Ti_{1-x}Sc_xOCl$ provided indications of a glassy magnetic state,[24] more recent measurements suggest that $\chi(T)$ can be modeled by finite chains of Heisenberg $S=1/2$ moments.[16] The presence of a large Curie tail at low temperatures is consistent with the freeing of spin 1/2 moments due to the disruption of singlet pairs by impurities.[16,24] To date, no evidence of coexisting antiferromagnetic order has been detected down to 2 K even in samples containing up to 3% Sc.[25] This result is particularly intriguing given that antiferromagnetic order has been observed in lightly doped $Cu_{1-x}Zn_xGeO_3$, with x as low as 0.0011,[10] and some theoretical models predict that long-range antiferromagnetic order should arise in disordered spin-Peierls systems for arbitrarily small dopings.[26]

In this paper we present x-ray scattering measurements on single-crystal $Ti_{1-x}Sc_xOCl$ which show this unconventional spin-Peierls ground state to be very sensitive to the presence of quenched, nonmagnetic Sc impurities even at concentrations on the order of only 1%. Sc doping suppresses the commensurate dimerization fluctuations observed in the incommensurate spin-Peierls and pseudogap phases of the pure material[27] and inhibits the formation of a commensurate long-range ordered state down to the lowest temperatures measured (~7 K). A short-range ordered, incommensurately modulated state is found at all temperatures below $\sim T_{c2}$.

II. EXPERIMENTAL DETAILS

Single-crystal samples of TiOCl, $Ti_{0.99}Sc_{0.01}OCl$, and $Ti_{0.97}Sc_{0.03}OCl$ were prepared using the chemical vapor transport method, as described in Ref. 16. The dimensions of the pure TiOCl sample were approximately $2.0\times2.0\times0.1$ mm^3, while the 1% and 3% Sc-doped samples were roughly $2.0\times1.0\times0.1$ and $1.0\times1.0\times0.1$ mm^3 in size, respectively. Samples were mounted on the cold finger of a closed cycle refrigerator and aligned within a Huber four circle diffractometer. The temperature stability of the samples was maintained at $\sim\pm0.01$ K. X-ray scattering measurements were performed using Cu $K\alpha$ radiation ($\lambda=1.54$ Å) produced by an 18 kW rotating anode source with a vertically focused pyrolytic graphite monochromator.

X-ray scattering scans were carried out at several equivalent commensurate ordering wave vectors $(H,K+1/2,L)$, where superlattice Bragg peaks are expected to arise as the result of spin-Peierls dimerization. These scans ultimately focused at the (2, 1.5, 1) position in reciprocal space, as it was here that the observed superlattice peak intensities were found to be strongest. Scans of the form (H, 1.5, 1), (2, K, 1), and (2, 1.5, L) were performed in the H, K, and L directions of reciprocal space, respectively. A high-temperature background data set, collected at 150 ($Ti_{0.99}Sc_{0.01}OCl$ and $Ti_{0.97}Sc_{0.03}OCl$) or 200 K (TiOCl), was then subtracted from each scan. This was necessary due to weak $\lambda/2$ contamination of the incident beam, which results in higher order Bragg scattering at the commensurate (2, 1.5, 1) position. This $\lambda/2$ scattering is comparable in strength to the incommensurate scattering observed in the doped samples (~0.1 counts/s), however, due to its lack of temperature dependence it can easily be eliminated by a simple background subtraction.

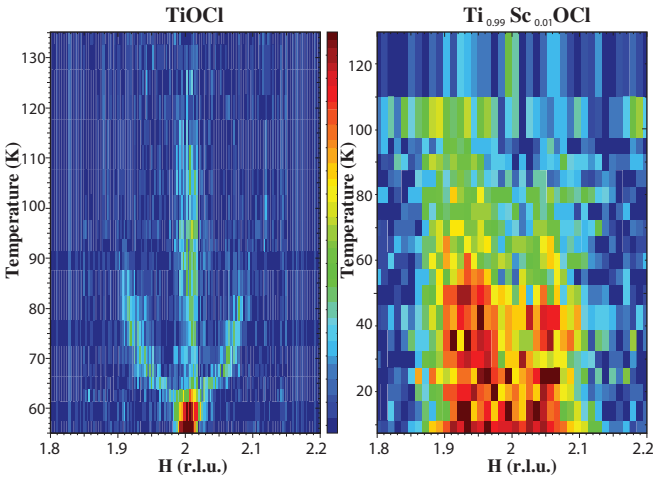

FIG. 1. (Color) Color contour maps of x-ray scattering as a function of temperature in $Ti_{1-x}Sc_xOCl$, with $x=0$ (left) and $x=0.01$ (right). These maps are composed of H scans of the form (H, 1.5, 1), as shown in Fig. 2, from which a high-temperature background scan has been subtracted.

III. RESULTS AND DISCUSSION

Figure 1 shows a comparison of the observed scattering in TiOCl and $Ti_{0.99}Sc_{0.01}OCl$. The two color contour maps illustrate the temperature dependence of H scans performed through (2, 1.5, 1) in both the pure and Sc-doped samples. It is evident that the introduction of quenched nonmagnetic impurities, even at the 1% level, has a profound effect on the spin-Peierls behavior of TiOCl. In the pure compound, the growth of commensurate dimerization fluctuations can be observed throughout the pseudogap phase from $T^*\sim130$ K to $T_{c2}\sim93$ K. In the incommensurate spin-Peierls phase, between T_{c2} and $T_{c1}\sim63$ K, these fluctuations compete and coexist with incommensurate satellite peaks which arise at $(2\pm\delta,1.5,1)$. At T_{c1}, the system locks into a commensurate long-range ordered spin-Peierls phase, which is maintained to low temperatures. In contrast, $Ti_{0.99}Sc_{0.01}OCl$ shows no sign of commensurate fluctuations in either the pseudogap or incommensurate spin-Peierls phases, and there is no evidence of commensurate long-range order down to ~7 K. As in the pure material, incommensurate scattering is found to develop in the doped compound near $T_{c2}\sim93$ K. However, the incommensurate scattering in $Ti_{0.99}Sc_{0.01}OCl$ is dramatically broader than that of TiOCl and there is no lock-in transition to a commensurate state near T_{c1}. Hence, a short-range ordered incommensurate phase is observed at all temperatures below T_{c2}.

Representative H scans for $Ti_{1-x}Sc_xOCl$, with $x=0$, 0.01, and 0.03, from which the color contour map in Fig. 1 was made, are shown in Fig. 2. The H scan for TiOCl was taken at $T=75$ K in the middle of the incommensurate spin-Peierls phase. This scan clearly demonstrates the coexistence of

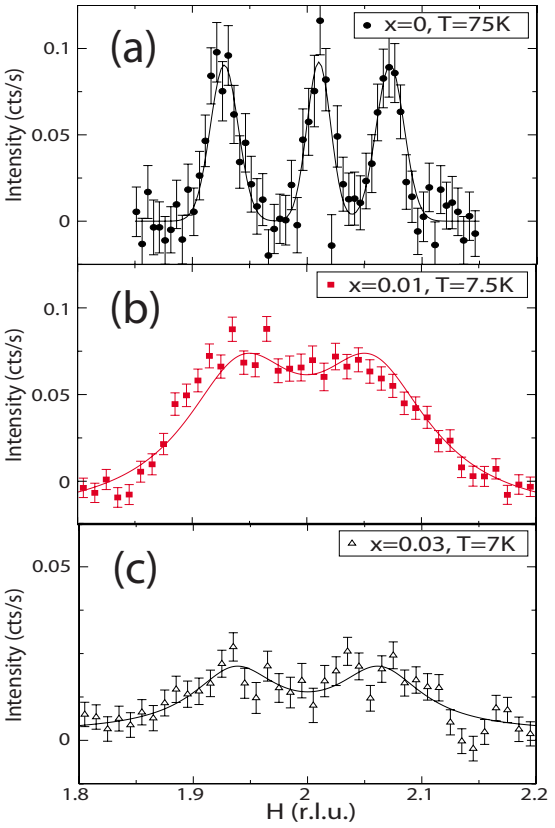

FIG. 2. (Color online) Representative H scans of the form (H, 1.5, 1) in $Ti_{1-x}Sc_xOCl$. Scans taken in the incommensurate spin-Peierls phases of (a) TiOCl at 75 K, (b) $Ti_{0.99}Sc_{0.01}OCl$ at 7.5 K, and (c) $Ti_{0.97}Sc_{0.03}OCl$ at 7 K. The solid lines represent fits to Eqs. (1) and (2), as described in the text.

commensurate and incommensurate scattering between T_{c1} and T_{c2}. The H scans for the $x=0.01$ and 0.03 samples were collected at base temperature ($T\sim 7.5$ and 7 K, respectively), where the dimerization scattering is fully developed. Since the H width of the incommensurate peaks in the doped samples is approximately equal to the magnitude of the incommensurate modulation wave vector, it is difficult to determine whether the scattering at the commensurate position is merely reduced or completely absent. However, an upper bound can be placed on the relative intensity of the commensurate scattering, which must be more than a factor of 15 times weaker in $Ti_{0.99}Sc_{0.01}OCl$ than TiOCl. The K and L scans which we performed showed no significant temperature dependence in either the peak width or the peak position. The experimental resolution was sufficiently broad in the K direction that the secondary incommensuration reported for TiOCl at ($H\pm\delta$, $K\pm\epsilon$, L) (Refs. 18 and 19) is expected to be unobservable. Thus, our measurements are sensitive to the component of the incommensurate modulation perpendicular to the dimerized chains (δ) but not the component which lies parallel to the chain direction (ϵ).

The data shown in Fig. 2 were fit to appropriate forms, allowing the incommensurate ordering wave vectors and correlation lengths to be extracted as a function of temperature for $Ti_{1-x}Sc_xOCl$. For pure TiOCl, such fits employed three Lorentzian peaks and a one-dimensional resolution convolution, suitable for near-long-range ordered line shapes, as shown in Fig. 2(a). For the $x=0.01$ and $x=0.03$ samples, fits were performed using a simple two peak model with Lorentzian line shapes. Since the widths of the incommensurate peaks in the doped samples are extremely broad, as shown in Figs. 2(b) and 2(c), no resolution convolution was necessary. The relevant two and three peak fit functions employed were

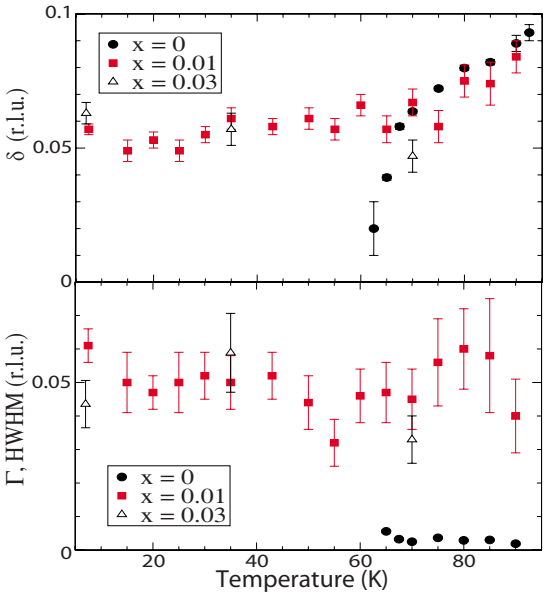

FIG. 3. (Color online) The temperature dependence of the incommensurate ordering wave vector, δ (top), and H width of the incommensurate scattering, Γ (bottom), in $Ti_{1-x}Sc_xOCl$. These parameters were determined from fitting the data in Figs. 1 and 2, as described in the text.

$$I_{\text{two peak}}(H) = A\left[\frac{1}{\left(\frac{H-2+\delta}{\Gamma}\right)^2+1}+\frac{1}{\left(\frac{H-2-\delta}{\Gamma}\right)^2+1}\right], \quad (1)$$

$$I_{\text{three peak}}(H) = I_{\text{two peak}}(H)+\frac{B}{\left(\frac{H-2+\delta_2}{\Gamma_2}\right)^2+1}, \quad (2)$$

where δ is the incommensurate ordering wave vector and $\Gamma=a/(2\pi\xi)$ is the half width at half maximum and the inverse correlation length.

The temperature dependence of the incommensurate ordering wave vector (δ, 0.5, 0) is shown in the top panel of Fig. 3. Between T_{c1} and T_{c2}, the behavior of δ is remarkably similar in both pure and Sc-doped TiOCl. In each case, the incommensurate wave vector reaches a maximum value of $\delta\sim 0.08$ near T_{c2} and decreases monotonically as the temperature approaches T_{c1}. At T_{c1}, however, δ drops rapidly to zero in TiOCl as the dimerization locks into a commensurate state, while δ remains constant at ~ 0.055 down to base temperature in $Ti_{0.99}Sc_{0.01}OCl$ and $Ti_{0.97}Sc_{0.03}OCl$. This clearly illustrates that while doping strongly suppresses the transi-

tion to the commensurate dimerized state, the mechanism driving the formation of the incommensurate dimerized state remains relatively unperturbed.

The origin of the incommensurate spin-Peierls phase in TiOCl has been attributed[20] to frustrated interchain interactions arising from competition between in-phase and out-of-phase dimer configurations within the bilayer structure. In this scenario, the stability of the incommensurate phase in $Ti_{0.99}Sc_{0.01}OCl$ and $Ti_{0.97}Sc_{0.03}OCl$ implies that the presence of nonmagnetic impurities alters the balance between intrachain and interchain interactions, favoring the frustrating interchain interactions along **a**.

The width of the incommensurate scattering, shown in the bottom panel of Fig. 3, is inversely proportional to the correlation length, ξ. Thus, the dramatic broadening of the incommensurate scattering observed in the H scans of the $x=0.01$ and $x=0.03$ samples indicates very short correlation lengths along the crystallographic a axis, ξ_a. Whereas the typical correlation lengths associated with the incommensurate long-range order in TiOCl are $\sim$200 Å, those for $Ti_{0.99}Sc_{0.01}OCl$ and $Ti_{0.97}Sc_{0.03}OCl$ are much shorter, on the order of $\sim$12 Å or three unit cells. We also note that ξ_a is temperature independent in the disordered $Ti_{1-x}Sc_xOCl$ and shows little or no variation between $x=0.01$ and $x=0.03$.

While doping is certainly expected to reduce the size of correlation lengths in the spin-Peierls state, this change in ξ_a is unusual in two respects. If one considers a simple scenario in which impurities are assumed to break dimerized chains by disrupting nearest-neighbor and next-nearest-neighbor interactions within the Ti-O bilayers, then $x=0.01$ and $x=0.03$ dopings should limit ξ_a to approximately 76 and 25 Å, respectively. The observed correlation lengths of $\xi_a \sim 12$ Å are somewhat surprising then, in that they are a factor of 2–6 times shorter than expected, and exhibit no discernable doping dependence. This implies that the disruption of spin-Peierls correlation lengths in $Ti_{1-x}Sc_xOCl$ is considerably stronger than our simple picture predicts and that the effect is almost fully developed by a doping of $x=0.01$.

The integrated intensity of the x-ray scattering around the commensurate (2, 1.5, 1) superlattice peak position is shown for pure and Sc-doped TiOCl in Fig. 4. These intensities come from Q integration of H scans through the (2, 1.5, 1) position, as shown in Figs. 1 and 2. The range of integration has been chosen to include both the commensurate and incommensurate ordering wave vectors, ensuring that all relevant dimerization scattering is captured. In TiOCl, this integrated scattering evolves continuously from T^* to T_{c1}, growing linearly with decreasing temperature. Below T_{c1} the integrated intensity saturates, coinciding with the development of commensurate long-range spin-Peierls order. In the $x=0.01$ and $x=0.03$ samples, the integrated intensity begins to increase near T_{c2} rather than T^*, and saturation occurs considerably lower than T_{c1}, between 40 and 50 K. The magnitude of the integrated scattering exhibits a pronounced doping dependence, as is evident from the rapid drop in observed scattering intensities that occurs with increasing x.

As the intensity of the superlattice dimerization scattering is proportional to the square of the relevant atomic displacements, a comparison of peak intensities can be used to determine the influence of impurities on the size of the spin-Peierls dimerization. The low-temperature saturation value of the integrated intensity near (2, 1.5, 1) is taken as the measure of the superlattice dimerization scattering in each of the three samples. In order to normalize the observed scattering intensities with respect to sample volume, the weak (2, 1, 2) structural Bragg peak is used as a reference. The structure factor for each reflection can be calculated from the expression $F=\sqrt{I \sin 2\theta}$, where I is the integrated intensity of the observed scattering and θ is the scattering angle. The relative magnitudes of the atomic displacements can then be found by comparing the ratio of $F_{obs}(2,1.5,1)/F_{obs}(2,1,2)$ for the $x=0$, $x=0.01$, and $x=0.03$ samples, as shown in the inset to Fig. 4. These results imply that for impurity concentrations as low as 1%, the dimerizing displacements are less than half the size of those observed in the pure material. A similar effect has been reported for Zn doping in $Cu_{1-x}Zn_xGeO_3$,[8] however the x dependence in $Ti_{1-x}Sc_xOCl$ is almost twice as strong.

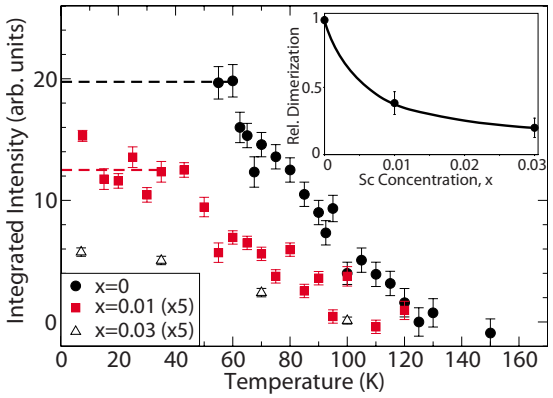

FIG. 4. (Color online) Temperature dependence of the integrated intensity of x-ray scattering in $Ti_{1-x}Sc_xOCl$. All intensities were obtained by integrating over H scans of the form (H, 1.5, 1) (as shown in Figs. 1 and 2). The intensities of the $x=0.01$ and 0.03 samples have been scaled by a factor of 5. The inset shows the x dependence of the relative spin-Peierls dimerization determined from a comparison of the integrated scattered intensities. All lines are intended as guides for the eyes.

Sc impurities are likely to perturb both the magnetic and elastic properties of TiOCl. In addition to creating finite spin chains and uncompensated spin 1/2 moments, substitution of Sc^{3+} ($r=0.745$ Å) for Ti^{3+} ($r=0.67$ Å) will also give rise to lattice strain and local distortions. These lattice effects may be particularly significant since it has been suggested that the frustrating interchain interaction in TiOCl, potentially the source of the incommensurate spin-Peierls phase, is predominantly elastic rather than magnetic in nature.[28] In doped $CuGeO_3$ differences in ionic radii are clearly important in disrupting spin-Peierls order. Substituting Si^{4+} ($S=0$, $r=0.42$ Å) for Ge^{4+} ($S=0$, $r=0.52$ Å) depresses T_{SP} two to three times more rapidly than doping either Zn^{2+} ($S=0$, $r=0.74$ Å) or Mg^{2+} ($S=0$, $r=0.72$ Å) onto Cu^{2+} ($S=1/2$, $r=0.72$ Å) sites.[7,9] Dopant size effects have also been shown to impact the critical properties of the spin-Peierls transition even resulting in changes in universality class.[11]

Figure 5 shows the normalized x-ray scattering intensity, $i=I/I_{saturation}$, as a function of normalized temperature, t

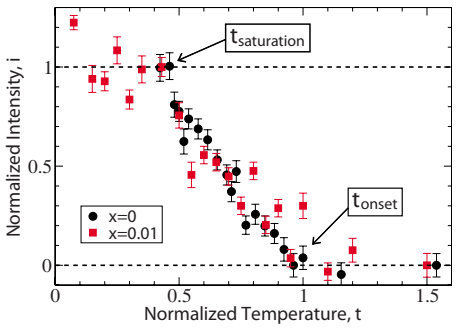

FIG. 5. (Color online) Normalized x-ray scattering intensity, $i = I/I_{\text{saturation}}$, as a function of normalized temperature, $t = T/T_{\text{onset}}$, in TiOCl and $Ti_{0.99}Sc_{0.01}OCl$. The onset of dimerization scattering occurs at approximately $T_{\text{onset}} \sim 130$ K for $x=0$ and $T_{\text{onset}} \sim 100$ K for $x=0.01$. All lines are intended as guides for the eyes.

$= T/T_{\text{onset}}$, in TiOCl and $Ti_{0.99}Sc_{0.01}OCl$. Here the integrated scattering intensities displayed in Fig. 4 have been rescaled with respect to their low-temperature saturation values, $I_{\text{saturation}}$, and the temperature ranges have been rescaled with respect to the first onset of dimerization scattering upon cooling, T_{onset}. In the case of TiOCl we have taken T_{onset} to be $T^* \sim 130$ K, the temperature at which commensurate dimerization fluctuations initially arise, while for $Ti_{0.99}Sc_{0.01}OCl$ we have chosen T_{onset} near T_{c2} at ~ 100 K, the temperature at which the earliest indications of incommensurate scattering appear. Thus, the data provided in Fig. 5 describe how each system evolves from the point at which dimerization (either static or fluctuating) first originates to the point at which the dimerization becomes fully developed. Note that when scaled in this fashion, both the $x=0$ and $x=0.01$ data sets appear to follow a common linear trend, reaching saturation at roughly $t \sim 0.45$. This correspondence is quite remarkable given that the nature of the dimerization is dramatically different in the TiOCl and $Ti_{0.99}Sc_{0.01}OCl$ samples.

As discussed earlier in this paper, one of the most striking similarities between the measurements performed on the $x=0$ and $x=0.01$ samples is that the transition to the incommensurate spin-Peierls phase occurs at almost exactly the same temperature, near $T_{c2} \sim 93$ K. This result would seem to contradict the wealth of experimental evidence from doped $CuGeO_3$ which shows that the introduction of impurities leads to consistent lowering of the spin-Peierls transition temperature, T_{SP}.[5–9,12,13] However, while Sc doping may not alter T_{c2}, it does produce a substantial drop in the onset temperature and saturation temperature of the spin-Peierls dimerization. Between $x=0$ and $x=0.01$ the values of T_{onset} and $T_{\text{saturation}}$ decrease by approximately 25%, an effect very similar in size to the suppression of T_{SP} reported for doped $CuGeO_3$ (typically between 15%–45% of T_{SP} for every 1% of dopants added to the system). These observations suggest that the most fundamental temperature scale for the spin-Peierls behavior in TiOCl and $Ti_{1-x}Sc_xOCl$ is not defined by the phase transitions at T_{c1} and T_{c2} but rather by the appearance and development of the dimerizing lattice displacement.

IV. CONCLUSIONS

In conclusion, we have shown that quenched nonmagnetic Sc impurities suppress commensurate spin-Peierls order and fluctuations in $Ti_{1-x}Sc_xOCl$ even at the $x=0.01$ level. A short-range ordered, incommensurate state arises near T_{c2} of the pure material, and this state is maintained down to the lowest temperatures measured (~ 7 K). The stability of the incommensurate spin-Peierls state, together with the absence of phase coexistence between T_{c1} and T_{c2}, suggests that Sc doping acts to effectively enhance the strength of frustrating interchain interactions within the Ti-O bilayers. The presence of Sc impurities also serves to break up one-dimensional dimer chains, dramatically decreasing the characteristic correlation lengths of the spin-Peierls state. In addition, Sc doping is found to severely affect the properties of the dimerizing atomic displacements which are associated with the formation of the spin-Peierls state, reducing both the average size of the dimerization and the temperature at which it first occurs. We hope that this work may guide and inform future theoretical and experimental studies of the doped titanium oxyhalide systems.

ACKNOWLEDGMENTS

The authors would like to acknowledge helpful discussions with T. Imai, A. Aczel, and J. Ruff. This work was supported by NSERC and NSCT.

[1] See, for example: E. Dagotto and T. M. Rice, Science **271**, 618 (1996); *Dynamical Properties of Unconventional Magnetic Systems*, NATO Advanced Studies Institute, Series E: Applied Sciences Vol. 349, edited by A. T. Skjeltorp and D. Sherrington (Kluwer, Boston, 1998).

[2] J. W. Bray, L. V. Interrante, I. S. Jacobs, and J. C. Bonner, in *Extended Linear Chain Compounds*, edited by J. S. Miller (Plenum, New York, 1983), Vol. 3, p. 353, and references therein.

[3] B. van Bodegom, B. C. Larson, and H. A. Mook, Phys. Rev. B **24**, 1520 (1981); M. D. Lumsden and B. D. Gaulin, *ibid.* **59**, 9372 (1999), and references contained therein.

[4] M. Hase, I. Terasaki, and K. Uchinokura, Phys. Rev. Lett. **70**, 3651 (1993); J. P. Pouget, L. P. Regnault, M. Ain, B. Hennion, J. P. Renard, P. Veillet, G. Dhalenne, and A. Revcolevschi, *ibid.* **72**, 4037 (1994).

[5] M. Hase, I. Terasaki, Y. Sasago, K. Uchinokura, and H. Obara, Phys. Rev. Lett. **71**, 4059 (1993).

[6] S. B. Oseroff, S. W. Cheong, B. Aktas, M. F. Hundley, Z. Fisk, and L. W. Rupp, Jr., Phys. Rev. Lett. **74**, 1450 (1995).

[7] J. P. Schoeffel, J. P. Pouget, G. Dhalenne, and A. Revcolevschi, Phys. Rev. B **53**, 14971 (1996).

[8] M. C. Martin, M. Hase, K. Hirota, G. Shirane, Y. Sasago, N. Koide, and K. Uchinokura, Phys. Rev. B **56**, 3173 (1997).

[9] B. Grenier, J.-P. Renard, P. Veillet, C. Paulsen, G. Dhalenne, and A. Revcolevschi, Phys. Rev. B **58**, 8202 (1998).

[10] K. Manabe, H. Ishimoto, N. Koide, Y. Sasago, and K. Uchi-

nokura, Phys. Rev. B **58**, R575 (1998).
[11] M. D. Lumsden, B. D. Gaulin, and H. Dabkowska, Phys. Rev. B **58**, 12252 (1998); S. Haravifard, K. C. Rule, H. A. Dabkowska, B. D. Gaulin, Z. Yamani, and W. J. L. Buyers, J. Phys.: Condens. Matter **19**, 436222 (2007).
[12] T. Masuda, A. Fujioka, Y. Uchiyama, I. Tsukada, and K. Uchinokura, Phys. Rev. Lett. **80**, 4566 (1998); Y. J. Wang, V. Kiryukhin, R. J. Birgeneau, T. Masuda, I. Tsukada, and K. Uchinokura, *ibid.* **83**, 1676 (1999).
[13] P. E. Anderson, J. Z. Liu, and R. N. Shelton, Phys. Rev. B **56**, 11014 (1997).
[14] M. Shaz, S. van Smaalen, L. Palatinus, M. Hoinkis, M. Klemm, S. Horn, and R. Claessen, Phys. Rev. B **71**, 100405(R) (2005).
[15] T. Sasaki, M. Mizumaki, T. Nagai, T. Asaka, K. Kato, M. Takata, Y. Matsui, and J. Akimitsu, J. Phys. Soc. Jpn. **74**, 2185 (2005).
[16] A. Seidel, C. A. Marianetti, F. C. Chou, G. Ceder, and P. A. Lee, Phys. Rev. B **67**, 020405(R) (2003).
[17] T. Imai and F. C. Chou, arXiv:cond-mat/0301425 (unpublished); S. R. Saha, S. Golin, T. Imai, and F. C. Chou, J. Phys. Chem. Solids **68**, 2044 (2007).
[18] A. Krimmel, J. Strempfer, B. Bohnenbuck, B. Keimer, M. Hoinkis, M. Klemm, S. Horn, A. Loidl, M. Sing, R. Claessen, and M. v. Zimmermann, Phys. Rev. B **73**, 172413 (2006).
[19] E. T. Abel, K. Matan, F. C. Chou, E. D. Isaacs, D. E. Moncton, H. Sinn, A. Alatas, and Y. S. Lee, Phys. Rev. B **76**, 214304 (2007).
[20] R. Ruckamp, J. Baier, M. Kriener, M. W. Haverkort, T. Lorenz, G. S. Uhrig, L. Jongen, A. Moller, G. Meyer, and M. Gruninger, Phys. Rev. Lett. **95**, 097203 (2005).
[21] J. Hemberger, M. Hoinkis, M. Klemm, M. Sing, R. Claessen, S. Horn, and A. Loidl, Phys. Rev. B **72**, 012420 (2005).
[22] P. J. Baker, S. J. Blundell, F. L. Pratt, T. Lancaster, M. L. Brooks, W. Hayes, M. Isobe, Y. Ueda, M. Hoinkis, M. Sing, M. Klemm, S. Horn, and R. Claessen, Phys. Rev. B **75**, 094404 (2007).
[23] H. Schafer, F. Wartenpfuhl, and E. Weise, Z. Anorg. Allg. Chem. **295**, 268 (1958).
[24] R. J. Beynon and J. A. Wilson, J. Phys.: Condens. Matter **5**, 1983 (1993).
[25] T. Imai, E. Mehes, F. L. Ning, S. Golin, S. R. Saha, A. Aczel, J. Rodriguez, F. C. Chou, and G. M. Luke, Bull. Am. Phys. Soc. **52**(1), 333 (2007); http://meetings.aps.org/link/BAPS.2007.MAR.J15.6.
[26] H. Fukuyama, T. Tanimoto, and M. Saito, J. Phys. Soc. Jpn. **65**, 1182 (1996).
[27] J. P. Clancy, B. D. Gaulin, K. C. Rule, J. P. Castellan, and F. C. Chou, Phys. Rev. B **75**, 100401(R) (2007).
[28] A. Schonleber, S. van Smaalen, and L. Palatinus, Phys. Rev. B **73**, 214410 (2006).